Tar characteristics generated from a 10 kW_{th} chemical-looping biomass gasifier using steel converter slag as an oxygen carrier

(article starts on next page)

Full Length Article

Tar characteristics generated from a 10 kW_{th} chemical-looping biomass gasifier using steel converter slag as an oxygen carrier

Fredrik Hildor [a],[*], Amir H Soleimanisalim [b], Martin Seemann [b], Tobias Mattisson [b], Henrik Leion [a]

[a] Chemistry and Chemical Engineering, Chalmers University of Technology, 412 93 Göteborg, Sweden
[b] Department of Space, Earth and Environment, Chalmers University of Technology, 412 93 Göteborg, Sweden

ARTICLE INFO

ABSTRACT

Tar management is one of the key components to achieve high energy efficiency and low operational costs connected to thermal gasification of biomass. Tars contain a significant amount of energy, and unconverted tars result in energy efficiency losses. Also, heavy tars can condense downstream processes, resulting in increased maintenance. Dual fluidized beds for indirect gasification operated with active bed material can be a way to better convert and control the tar generated in the process. Using an active material to transport oxygen in an indirect dual reactor gasification setup is referred to as chemical-looping gasification (CLG). A higher oxidative environment in the gas phase, in addition to possible catalytic sites, could mean lower yields in comparison to normal indirect gasification.

This paper investigates the effect of using Steel converter slag (LD slag), a byproduct of steel manufacturing, as an oxygen-carrying bed material on tar species generated in a 10 kW_{th} dual fluidized bed biomass gasifier. The results are compared to the benchmark oxygen carrier ilmenite and conventional silica sand. Three different solid biofuels were used in the reactor system: steam exploded pellets, pine forest residue and straw. Tar was absorbed from the raw syngas using a Solid Phase Adsorption (SPA) column and was analyzed using GC-FID. Bench-scale experiments were also performed to investigate benzene conversion of LD slag and ilmenite at different oxidation levels.

The findings of this study suggest that oxygen carriers can be used to decrease the tars generated in a dual fluidized bed system during gasification. Phases in LD slag possess catalytic properties, resulting in a decreased ratio of heavy tar components compared to both ilmenite and sand. Temperature and fuel load showed a significant effect on the tar generation compared to the circulation and steam ratio in this reactor system. Increased temperature generated lower tar yields and lower ratios of heavy tar components for LD slag in contrast to sand.

1. Introduction

Gasification of biomass provides the possibility to use fossil-free carbon for gaseous fuel production or synthesis of liquid fuels or products. It is also possible to produce heat and power simultaneously increasing the overall efficiency of the process. The gasification technology, although promising, needs to overcome many challenges to become viable. One of the most prominent issues is the formation of heavy hydrocarbons, named tar, which condense at relatively high temperatures and can cause operational issues. In addition, biomass tar can correspond to 5–10 % of the energy content of the fuel [1,2]. Biomass tars are formed by oxygenates and monoaromatics formed at low temperatures that mature by polymerization to unsubstituted polyaromatic hydrocarbons and eventually can become soot [3]. Limiting the amount of tar generated from the core process and which are transferred to downstream processes is one of the keys to the efficiency of the process.

Indirect gasification using a Dual Fluidized Bed (DFB) system has been observed as a promising large-scale technique for gasification [4,5]. The 20 MW DFB gasifier GoBiGas pilot plant was built in 2011–2012 and operated until 2018. Here the technique was demonstrated, revealing the opportunities and operational issues with the process. Among the most problematic technical issues was the tar generated, which required extended gas cleaning [6].

A similar process to the DFB gasifier is Chemical Looping Gasification (CLG) which utilizes an oxygen carrier instead of inert sand to both transport heat and oxygen to the gasifier. In Fig. 1 the CLG process is illustrated with a circulating oxygen carrier, M_xO_y, transferring oxygen from the air reactor to the gasifier. Oxygen transport to the fuel in the gasifier is normally related to direct gasification, so CLG can be seen as a combination of an indirect DFB gasifier and a direct gasifier. Besides oxygen transport, the oxygen carrier also transports heat to the endothermic gasification reaction, this is very important and needs to be considered when controlling the system [7]. The potential advantages of CLG technology are numerous. First of all, the technique is designed so that all raw syngas from the process are collected in one stream from the process, simplifying carbon capture [8,9]. If using biomass as a source of carbon, capturing CO_2 from the raw syngas generates net negative emissions [10]. Increased CO_2 can also promote char gasification. In addition, oxygen carriers can promote tar reforming [11]. A suggested explanation is that the concentration of inhibiting species around the char particles is lowered since they are converted by the oxygen carrier. Volatile species, in particular tar and hydrogen, have been shown to inhibit char gasification [11–14].

Larsson *et al.* [1] investigated the impact of using ilmenite in the Chalmers' 2–4 MW DFB gasifier to reduce the tar yield. Ilmenite was diluted with sand at different ratios for the experiments in the gasifier. It was reported that the total tar amount was decreased by ~50 % with only 12 wt% ilmenite in the bed. However, a significant decrease in cold gas efficiency was also observed in this work besides the decreased tar yield. In chemical looping applications, the iron–titanium oxide ore ilmenite has been considered as a benchmark oxygen carrier for biomass chemical looping [15,16], also promoted by the fact that it is used commercially in fluidized bed combustion processes [17]. Besides ilmenite, other iron-based oxygen carriers have been considered for these types of applications [15,18–21]. One of the iron-based oxygen carriers is Basic oxygen furnace slag, also called LD slag, which is a by-product of the steel manufacturing process. This is a by-product that is produced and has low demand on the market and is therefore available at a lower cost compared to ilmenite [19]. LD slag has been successfully operated in Chalmers 12MWth boiler [19] and has been observed to have similar reactivity as ilmenite both towards gaseous fuels and char in batch reactors [20,21] LD slag has been compared to ilmenite in a smaller continuous unit for chemical looping application. Here it was concluded that LD slag could be a relevant material due to the low cost, even though a higher attrition rate and little lower reactivity were observed for LD slag [22]. Further, LD slag was also used in a connected 2–4 MW DFB gasifier, and it was observed that a lower amount of tars

were generated compared to other bed materials [23]. LD slag is also known to not absorb alkali in the same way as silica sand and ilmenite, releasing more of the alkali in the gas phase [24]. Since gas phase alkali is known to have a catalytic effect on the conversion of tars [25–27], this ability of the bed material could be beneficial for tar conversion.

The 2–4 MW DFB gasifier referred to above, and used by e.g. Larsson *et al.* [1] is a bubbling fluidized bed (BFB) with a top feeding of fuel. Known for chemical looping processes operating with oxygen carriers and solid fuels, it is important to distribute the volatiles of the fuel in the reactor [28]. This distribution is needed to obtain a well fuel-oxygen carrier mix gaining a high conversion. In a top feed BFB, the mixture between bed material and fuel volatiles is often insufficient. Different designs of chemical looping reactors have been suggested to handle this mixing issue [29–31]. The newly recommissioned 10 kW_th chemical looping pilot reactor at Chalmers was equipped with a new submersed volatile distributor in the fuel reactor. It has been observed that this design increased the carbon conversion for volatile fuels compared to the earlier generation of the system. However, tars were not considered in this study [32].

In this study, the oxygen carriers LD slag and ilmenite, as well as the reference material, sand, were used as bed material in the recommissioned 10 kW_th chemical looping pilot reactor. e The 10 kW_th reactor was operated under CLG conditions with three different fuels. The study aimed to comprehensively investigate, at a pilot plant scale, if the oxygen carrier LD slag performs equally with the benchmark oxygen carrier ilmenite regarding tar conversion.

2. Material and methods

Two iron-based oxygen carriers were used for this study: LD slag and ilmenite ore. LD slag was provided by SSAB Sweden from their steel plants in Oxelösund, Sweden. The material had been stored outdoor and was crushed, dried, sieved and sent to Chalmers. Here the material was heat-treated for 4 h at 500 °C followed by 8 h at 950 °C in a box furnace. After the heat-treatment, the material was sieved again to obtain the size fraction of 125–400 μm. Ilmenite was provided by Titania AB in Norway and was a crushed rock ilmenite ore. It was heat-treated for 2 h at 500 °C followed by 12 h at 950 °C in a box furnace. The Ilmenite was hence sieved to obtain the size fraction 125–400 μm. As a reference case for gasification, sand was used as bed material. The sand was provided by Sibelco Nordic AB (Baskarp B28) and consisted primarily of SiO_2. The size distribution of the sand was 90–355 μm. Elemental analysis, see Table 1, of LD slag was performed using ICP- SFMS According to SS EN ISO 17294–2: 2016, ilmenite was analyzed with XRF - X-ray fluorescence (SP metod 4343).

For the experiments in the batch reactor, the same oxygen carrier material was used. The only difference was that both the materials were sieved to the size range of 150–400 μm and both were heat-treated for 24 h at 950 °C in a box furnace. During the experiments, 5 g oxygen carrier was blended with 10 g sand with the size range of 180–250 μm.

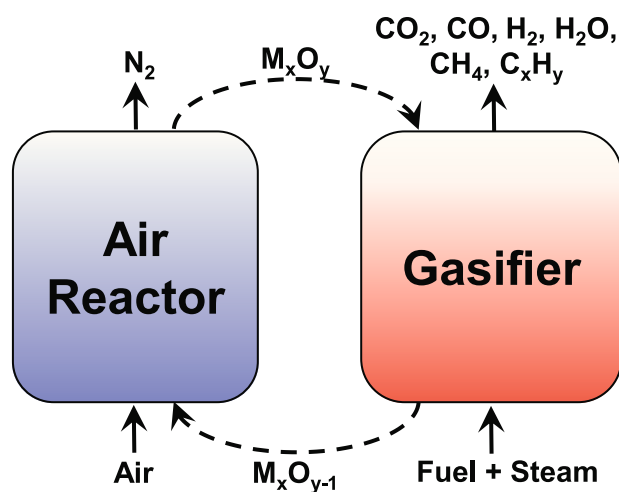For this study, three different solid fuels were used in the

Fig. 1. Schematic overview of the CLG process where an oxygen carrier containing a metal oxide (M_xO_y) transports oxygen from the air reactor to the gasifier.

Table 1
Elemental composition is given in wt.% of the studied bed materials excluding oxygen.

Element	LD slag	Ilmenite	Sand [33]
Fe	17	36	0.04
Ti	0.78	28	–
Ca	32	0.22	–
Si	5.6	0.67	46
Mg	5.9	2.0	–
Mn	2.6	0.21	–
V	1.5	0.12	–
Al	0.76	0.17	0.09
Cr	0.33	0.06	–
Ni	0.002	0.03	–

experimental campaigns at the 10 kW$_{th}$ dual fluidized bed reactor system: Black Pellets (BP), Pine Forest Residue (PFR) and Straw. The BP was steam exploded pellets provided by Arbaflame AS, Norway. The pellets were crushed to obtain the size of 0.7–2.8 mm. Pine Forest residue was provided by National Renewable Energy Centre (CENER), Spain. The PFR was crushed to obtain the size of 0.7–3.0 mm. Straw pellets were provided by Stohfelder, Austria. The straw was crushed to obtain a size fraction of 0.7–3.5 mm. Table 2 shows the fuel analysis performed according to commercial standards, and elemental analysis performed with ICP-OES.

For the experiments in the batch reactor, a synthetic gasification gas was used in a blend with benzene. The composition of this synthetic gasification gas can be seen in Table 3.

2.1. 10 kW$_{th}$ dual fluidized bed reactor – CLG reactor

The 10 kW$_{th}$ pilot plant is an electrically heated reactor system that 2019 was rebuilt [32]. The main changes was mainly that the carbon stripper was removed and that a new design of the fuel reactor (FR) was used for better volatile conversion. The general design of the reactor system can be seen in Fig. 2. The AR is a circulating bed where the bed is lifted in the AR Riser into the cyclone. The circulation of particles in the system is monitored by adjusting the airflow into the AR. Both the upper and lower loop seals are fluidized with nitrogen. The FR is a bubbling bed fluidized with steam. It is designed with porous plates submerged in the bubbling bed what's purpose is to distribute the volatiles from the fuel. The fuel is dropped down in the fuel chute where a screw transports the fuel from the fuel hopper. Fuel feed rates are controlled by the rotation speed of the screw. Fuel load calculations were based on the lower heating value and previous calculations on the fuel feeding rate from the screw. A vibrator was mounted on the fuel chute to prevent blocking of the fuel, the vibrator was operated for 5 s in a 30 s interval. Further details of this reactor system can be found elsewhere [32].

Bed materials are circulated in the system via the AR riser and are then transported through the following sections by gravity. Circulation of the bed material in the system was estimated using the parameter circulation index, CI. CI is calculated using equation E1, where $\Delta P_{AR\ riser}$ is the differential pressure in the AR riser given in kPa and $\dot{Q}_{air,AR}$ are the flow of air into AR given in nL/min [32].

$$CI = \Delta P_{ARriser} * \dot{Q}_{air,AR} \qquad (1)$$

The circulation of the oxygen carrier controls both oxygen transfer and heat transfer in a continuous CLG unit. Therefore, this parameter is important for operational control. In this unit, there is no post-

Table 2
Analysis of the fuel used in the 10 kW$_{th}$ pilot Chemical looping reactor. Values are given for as-received fuel.

Component	Unit(s)	Black pellets (BP)	Pine forest residue (PFR)	Straw
Moisture	%	5.7	9.2	8.8
Ash	%	0.3	1.8	7.9
Volatiles	%	74.2	80.0	67.5
Fixed C	%	19.8	9.0	15.8
C	%	49.6	46.9	42.0
H	%	6.5	5.7	6.1
N	%	<0.1	0.35	0.7
O	%	43.6	36.0	43.0
Si	mg/kg dry fuel	<530	–	19,000
Ca	mg/kg dry fuel	820	–	7700
K	mg/kg dry fuel	460	2080	11,000
Na	mg/kg dry fuel	<53	27	260
LHV	MJ/kg	18.7	18.0	15.1

Table 3
The gas composition is given in vol.% of the artificial gasification gas used in the laboratory fluidized bed reactor.

	CH$_4$	CO$_2$	CO	C$_2$H$_4$	H$_2$
Gasification gas	14	14.9	43	5	23.1

combustion chamber to facilitate the complete combustion of the raw syngas and char to determine the total coal balance. This leaves a high error in oxygen-to-fuel ratio (λ) calculations. The transport of oxygen from AR to FR was calculated using the oxygen consumption in the AR and was calculated to be given kgO$_2$/kWh for the different fuels. This value was corrected by the subtraction of oxygen consumed by char transport, forming CO$_2$ in the AR.

Cold gas efficiency was estimated from the concentrations of CO, CH$_4$ and H$_2$ in the outgoing gases, assuming that these gases contributed to the majority of the raw gas energy. This was then correlated to the lower heating value of the fuel, given in Table 2.

2.1.1. Tar measurements

Raw syngas were extracted from the FR chimney just above the furnace and sucked out into a heated line from the reactor using a venturi pump system. The line was heated to 350–375 °C. From this line, a 100 ml sample of raw syngas was extracted through a heated metallic filter with a mesh size of 7 μm to remove solid particles from the raw syngas. This extraction was done using a pneumatic pump system connected to the syringe that was pressed through a septum next to the heated metallic filter, see Fig. 3. The 100 ml sample gas was sucked through a SPA (Solid Phase Adsorption) column that should absorb the tars in the sample gas. The SPA column was Superclean^{TM} Envi-Carb^{TM}/LC-NH$_2$ 3 ml tubes delivered by Supelco. The method has been evaluated [34] and used in previous studies, e.g.[1,35].

Before every sample extraction, a blank sample was extracted with a SPA column that was discarded. This was to fill the filter and dead volume between the filter and septum with new raw syngas. Every sample was then extracted twice for each experimental condition, these duplicates were used to evaluate the stability of the method. The SPA columns and syringe were then sealed and directly cooled in an icebox. The SPA columns were then by the end of the day transported to a freezer at −20 °C and stored until elution was performed 1–2 days later.

Elution was performed using a standardized elution solution, "P-eluent", containing eight parts dichloromethane, one part isopropanol and one part acetonitrile. The first elution of the SPA columns was performed with 2.4 ml + 0.8 ml P-eluent. A small stream of nitrogen was used to push the solvent through the column. 75 μl internal standard (2 mg/ml 4-Ethoxyphenol dissolved in P-eluent) was added directly to the container. A second elution of the SPA column using 0.8 + 0.8 ml was performed to extract the remaining tar species from the column. To the second elution 75 μl internal standard was added to the elute. Also, the needle was eluted together with the SPA.

The elute from the SPA columns was analyzed using a Bruker GC430 connected to an FID detector using hydrogen as carrier gas. A 30 m midpolar column was used with a temperature program up to 340 °C. Every sample was analyzed three times and compared to an external standard containing: Benzene, Toluene, p-Xylene, o-Xylene, Styrene, Methylstyrene40, Methylstyrene60, Phenol, 2,3-benzo(b)furan, Indene, o-Cresol, p-Cresol, 1,2-dihydroNaphthalene, Naphthalene, 2-MethylNaphthalene, Intern standard, 1-MethylNaphthalene, Biphenyl, Acenaphthylene, Acenaphthene, Dibenzofuran, 1-naphtol, 2-naphtol, Fluorene, Xantene, Phenanthrene, Anthracene, Fluoranthene, Pyrene, Crysene/Triphenylene. These components are grouped into 1-ring, 2-ring, 3-ring and 4-ring compounds depending on the number of aromatic carbon rings the compound contains.

The tar concentrations are given as g/m$_{dg}^3$ and are therefore affected by the amount of dry gas generated from the fuel reactor. The dry gas flow was estimated over a 5 min period of stable operation before the tar
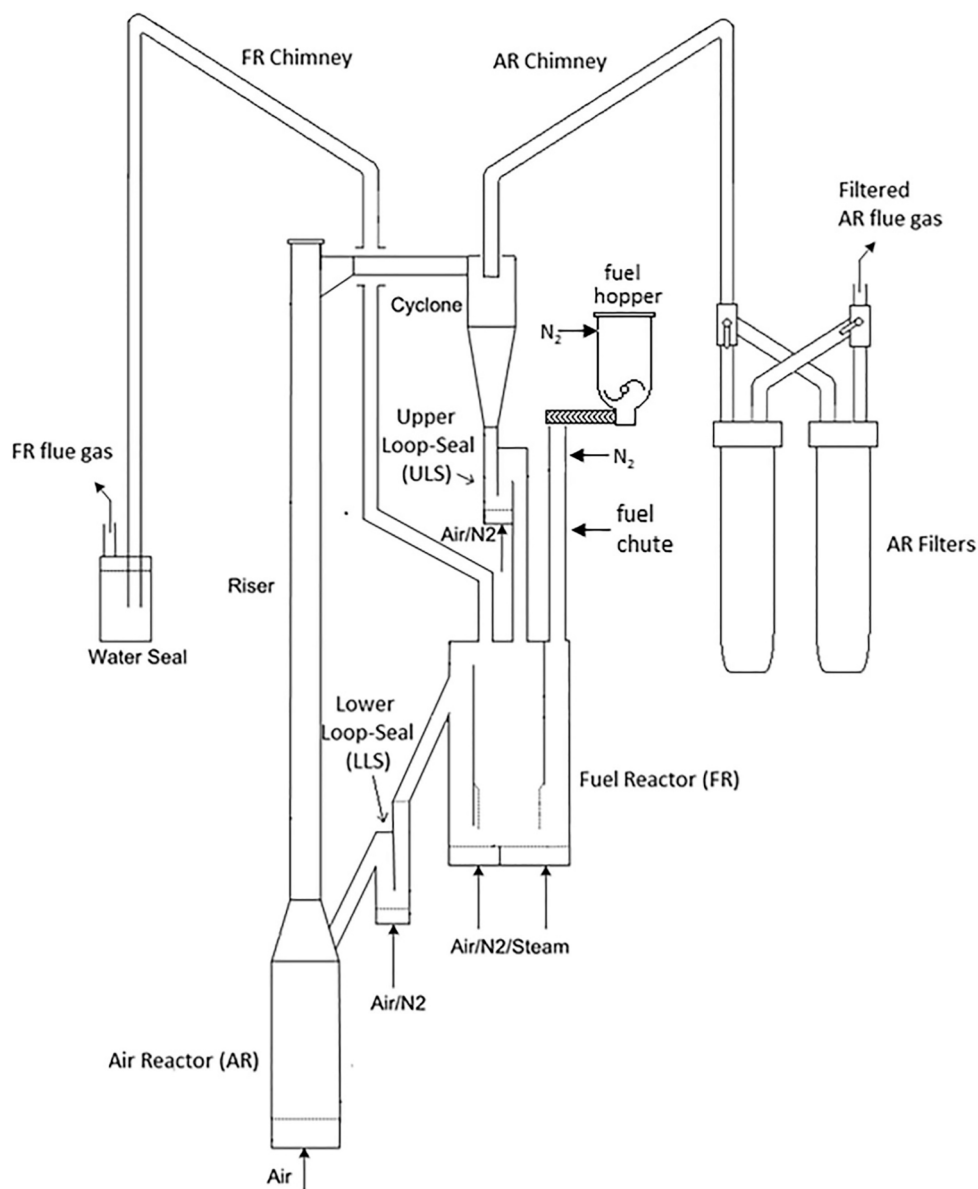
Fig. 2. The layout of the 10 kW$_{th}$ solid fuel chemical looping reactor system [32].
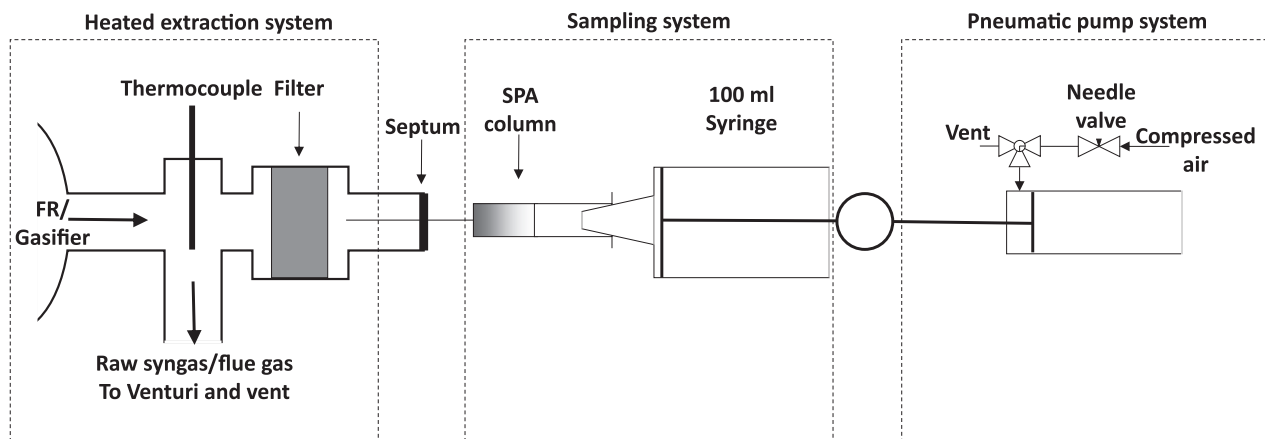

Fig. 3. The entire tar sampling system. Left: Heated system where the raw syngas is extracted from the Fuel Reactor (FR). Middle: The sampling system where a needle pierces a septum to extract 100 ml filtered hot raw syngas containing tars that are absorbed in the SPA column. Right: The Pneumatic pump system was used to control the syringe to extract with the same suction rate for every sample.

sampling. It is assumed that the measured concentrations of CO, CO_2, CH_4, H_2 and O_2 are the majority of the gases besides N_2. Nitrogen in the FR-raw syngas originates from the sweep gas with fuel, upper and lower loop seal, and pressure taps. Assuming that 50 % of the flow from either loop seal enters the FR raw syngas and that a constant flow of 1 L_N/min from the pressure tap, equation E2 can be used to estimate total dry gas FR raw syngas flow.

$$\dot{V}_{dg,FR} = \frac{\dot{V}_{N_2,tot}}{1 - x_{CO_2,FR} - x_{CO.FR} - x_{H_2,FR} - x_{CH_4,FR} - x_{O_2,FR}} \quad (2)$$

From the tar amount in the dry gas, the total dry gas flow and the fuel load, the amount of tar (tar yield) could be calculated to be given in g/kWh.

2.2. Laboratory fluidized bed reactor

A laboratory fluidized bed reactor was used to investigate the reactivity of oxygen carriers towards the tar model molecule benzene. Benzene was used as a model tar since it is the simplest aromatic compound and high benzene concentrations were observed in the 10 kW$_{th}$ experiments. The layout of the reactor system can be seen in Fig. 4. To the left the gas monitoring, mixing and selection system are seen. Magnetic valves are used to select the desired gas which is introduced to the reactor. The magnetic valves are always open towards either the reactor or ventilation, which facilitates stable and continuous gas flows and less transients during gas-switching. Steam is generated by injection of Milli-Q water into an emulsion evaporator system heated to 150 °C together with nitrogen. Benzene was inserted into the system by bubbling room temperature N_2 through a beaker containing benzene. This gas blend was then cooled at 6 °C to generate a saturated gas with 4.86 % benzene.

The gas then flows through heated lines at the bottom of a quartz reactor with a diameter of 22 mm. The quarts reactor is mounted inside a furnace to monitor the temperature. In the quartz reactor, a porous quart's plate is installed. On this porous plate, the sample of bed material is placed. Temperature is measured both below the porous plate and in the bed with a quartz-protected K-type thermocouple. The pressure fluctuations over the reactor are measured in the inlet and outlet with a Honeywell pressure transducer with a frequency of 20 Hz.

Downstream the reactor an FTIR analyzer was mounted to analyze the hot wet gases, where benzene and steam were measured. The gas lines were electrically heated above 100 °C. Thereafter, a cooler to condense and separate steam was mounted. The dry gas was then

analyzed using a Rosemount NGA 2000 equipped with IR/UV sensors for CO, CO_2 and CH_4, and a thermal conductivity sensor for H_2 and a paramagnetic gas sensor for O_2. More information regarding the reactor system can be found elsewhere [36].

2.2.1. Experimental procedure

A bed containing 5 g oxygen carrier and 10 g sand was exposed periodically to different atmospheres. First, the oxygen carrier was fully oxidized i.e. exposed to an atmosphere of 5 % O_2 until the oxygen carrier cannot absorb more oxygen. Then an inert purge with N_2 was introduced for 180 s. Thereafter, a reducing atmosphere containing either CO or steam, benzene and gasification gas was introduced for 60 s. Table 4 describes the different components of the reducing gas. Another inert purge for 180 s followed the reduction before the oxygen carrier was oxidized.

Three repetitions of each of the exposures were done at three different temperatures: 850 °C, 900 °C and 950 °C. The introduction of synthetic gasification gas containing 43 % CO, 14.9 % CO_2, 14 % CH_4, 5 % C_2H_4, and 23.1 % H_2 was done to see the behavior of introduced inhabitants for tar conversion and selectivity of benzene conversion when other reducing species was present in the gas. The flow of the gasification gas was limited due to the generation of benzene vapors with N_2 and the steam generation.

For some exposures, the bed was pre-reduced for 5–20 s using the gas composition as described in Table 4. This pre-reduction followed by another intermediate purge with N_2 was done before the exposure of steam and benzene-containing mixture with no gasification gas. This was performed three times at 850 °C for every experiment with different pre-reduction time.

Table 4
Gas composition for reducing exposures in the laboratory batch fluidized bed.

Treatment notification	Exposure time [s]	Flow [ml/min]	Gas composition
20 % Gasification gas	60	1000	50 vol% steam, 20 vol% Gasification gas, 1.5 vol% Benzene, N_2 Balance
10 % Gasification gas	60	1000	50 vol% steam, 10 vol% Gasification gas, 1.5 vol% Benzene, N_2 Balance
0 % Gasification Gas	60	1000	50 vol% steam, 1.5 vol% Benzene, N_2 Balance
Pre-reduction	5 – 20	900	50 vol% CO in N_2
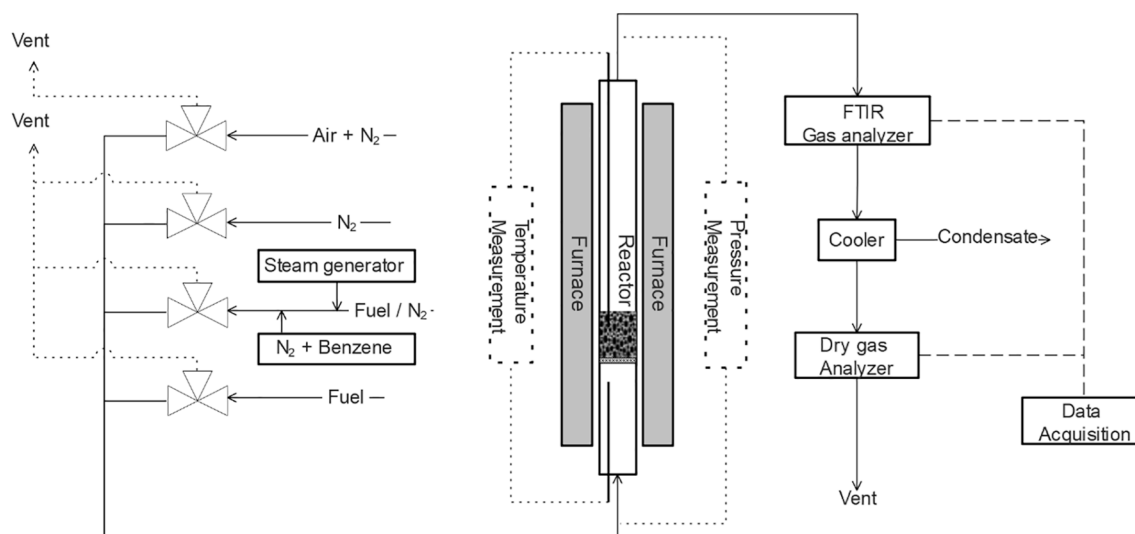
Fig. 4. Schematic layout over the batch reactor used for gasification experiments.

2.2.2. Data evaluation

Quantification of the outgoing gases from the batch reactor system was calculated as the molar flow multiplied by the concentration of the species integrated over time, see equation E3.

$$n_{i,t} = \int_{t_1}^{t_2} x_{i,out} * \dot{n}_{out} dt \qquad (3)$$

The conversion of a fuel species over a cycle, γ_{feul}, was determined by comparing the outgoing fuel species to the ingoing, see equation E4. The molar flow was calculated from the volumetric flow assuming ideal gas. For species measured in the FTIR under steam conditions, such as experiments with benzene, it was assumed that the molar flow was equal to the ingoing gas flow.

$$\gamma_{Fuel} = \int_{t_{red}=0}^{t_{red}=end} \frac{x_{Fuel,in} * \dot{n}_{in} - x_{Fuel,out} * \dot{n}_{out}}{x_{Fuel,in} * \dot{n}_{in}} dt * 100\% \qquad (4)$$

The oxidation state, ω, is defined by the mass of the oxygen carrier divided by the oxidized weight of the oxygen carrier, see equation E5. At a specific time, the mass of oxygen transferred to the fuel can be determined from the exhaust gases and the ω at the time t_i calculated. For a fuel only containing CO, equation E6 is used.

$$\omega = \frac{m}{m_{ox}} \qquad (5)$$

$$\omega_{t_i} = \omega_0 - \int_{t_0}^{t_i} \frac{\dot{n}_{out} M_O}{m_{ox}} (x_{CO_2}) \qquad (6)$$

To determine the oxidation level of the oxygen carrier at the end of the exposure, equation E7 was used. Here the oxygen absorption is calculated for an oxygen carrier in comparison to an inert material in the same experimental setup. The difference between the O_2 concentration are the absorbed oxygen into the oxygen carrier for one cycle.

$$O_{2,absorption} = \int_{t_{ox}=0}^{t_{ox}=end} (x_{O_2,ref} - x_{O_2,sample}) * \dot{n}_{out} \qquad (7)$$

3. Results

3.1. Operation in 10 kW_{th} CLG pilot reactor

3.1.1. Effect of oxygen carrier

During a CLG operation in the 10 kW_{th} pilot reactor, it was observed that the most pronoun species of tars were the unbranched 6-carbon ring aromatics. Benzene was by far the most pronoun species, followed by naphthalene and phenanthrene. This was observed for all bed materials, independent if having oxygen-carrying properties or not. It was only at the lower temperature of 870 °C, and with a high fuel load, that significant amounts of more branched compounds, such as phenol, were detected.

Fig. 5 shows the measured tar amounts for Sand, LD slag and Ilmenite used as bed materials for CLG operation in the 10 kW_{th} pilot system. Based on the results, the yield of tars, BTX (benzene, toluene and xylene) and higher aromatic carbon structures, were significantly lower for LD slag compared to ilmenite and sand operated in similar conditions. It was also noted that the ratio between higher carbons, 3-rings and 4-rings, in relation to the sum of BTX was highly affected by the oxygen carrier. The lowest amounts were observed for LD slag at 970 °C with PFR as fuel. Comparing the 4-ring/BTX ratio using different bed materials at 8 kW load, ilmenite and sand had roughly 3 and 10 times higher ratio than LD slag. For the 3-ring/BTX ratio at the same experiments, ilmenite had roughly 2 and sand 3 times higher ratio compared to LD slag. It can also be noted that the measurement for LD slag at 970 °C in Fig. 5 was sampled and measured 4 times (compared to the normally 2 samples) with a similar or lower tar amount every time.

It was observed that the amounts of unidentified peaks were lower for LD slag than for ilmenite and sand in the 10 kW_{th} system, see Fig. 5. Important to notice is that the unknowns are not quantified since they are not calibrated, the amount is only related to the area in the GC spectrum and can therefore only be compared to each other. Uniquely for ilmenite, one of the major unknown peaks was located at ~ 35 min in the GC chromatogram, a compound that had a slightly longer residence time in the GC column than Crysene/Triphenylene at both 870 °C and 970 °C. This unknown peak was present only when ilmenite was used as the bed material, and independent of the biomass fuel and contributed to more than 50 % of the unknown hydrocarbon amount in these tests. In comparison to the other tested materials, no significant peak could be observed after Crysene/Triphenylene.

Element migration due to cyclic redox reactions and ash interaction is known to affect and age oxygen carriers like ilmenite [37,38] and LD slag [20]. To see the effect of the oxygen carrier aging development, experiments were repeated after more than 11 h of fuel operation between the fourth and sixth day. Only 3.5 kg of fresh calcined LD slag was added to the reactor unit during this time due to material loss over time. Note that the operation the fourth day was not committed with fresh material, the material had already been used and fresh material had been added frequently before and operation performed with both PFR
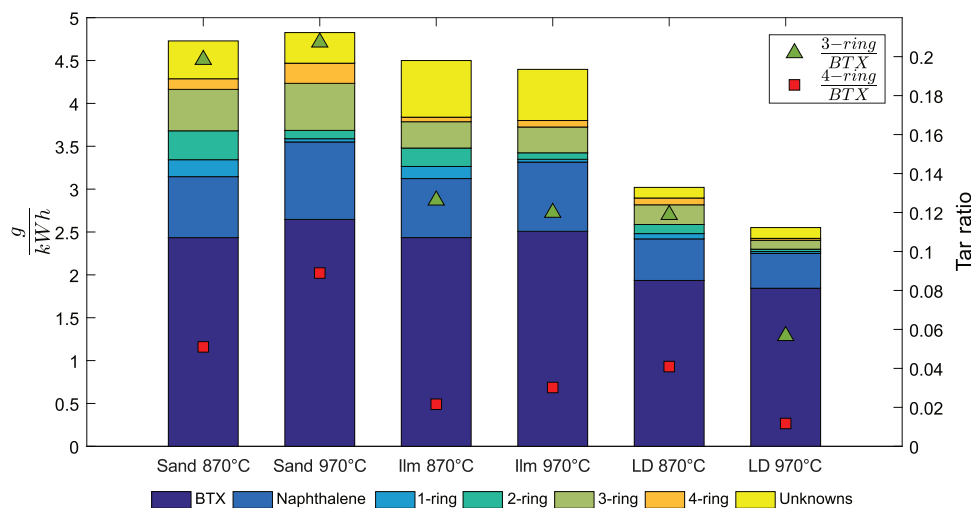

Fig. 5. Measured and identified tar amounts for Sand, LD slag and Ilmenite used as bed materials for CLG operation in the 10-kW_{th} chemical looping reactor operated with PFR fuel with a load of 8 kW. The ratios of identified 3-ring and 4-ring towards BTX were calculated and are marked in the figure.

and BP. The results can be seen in Fig. 6. Both the tar measurements are plotted to give an idea of the errors of the tar collection and then the same operational conditions are plotted for the two different days. Unfortunately, the oxygen transfer could not be calculated due to errors with oxygen measurements from the AR during one of the days. However, the cold gas efficiency, which theoretically are proportional to the oxygen transfer, was calculated and are given instead in the figure.

Fig. 6 indicates the stability of the tar measurement technique. The error for a single measurement can be considered to be relatively low. However, there is a clear effect of aging of the bed materials that needs to be considered when comparing results from the system. Comparing the PFR 970 °C 8 kW from the fourth and sixth day, even though the cold gas efficiency of the product gas is similar, the amount of detected tar species was greater for the later sample. Also, the amount of higher 3-ring and 4-ring tar species were higher in relation to BTX for more aged sample. Note that it is the higher level of tars from the 28/10 that is used in Fig. 5 in comparison with ilmenite and sand.

3.1.2. Effect of fuel and fuel load

Operation with LD slag as oxygen carrier using either PFR, BP or straw at different loads at 970 °C can be seen in Fig. 7. For both PFR and BP the amount of tar increased with increased load. However, the ratios between 3-ring and 4-ring tars towards BTX were roughly the same for all the loads. For straw, the amount of tar was unaffected by increasing the load, even if the $(H_2 + CO)/CO_2$ ratio increased. Since straw has a high amount of alkali and this is known to catalyze tar cracking [6,25,39], the fuel alkali content could be the reason for the comparable lower tar concentrations and that the tar generation is unaffected by the load.

It was observed that the fuel feeding system was affecting the tar sampling system. If the tar sample was taken at the same time as a vibration, more fuel was added, and more tar was generated compared to just taking a tar sample just before the vibration. This suggests that there is instability in the fuel feeding system, and this might affect the observed tar yields. All samples were extracted twice and most of the pairs had only a minor difference in the results, see examples in Fig. 6. Therefore, in this paper, only the second repeat or the sample with the highest tar yield was used for the comparison.

3.1.3. Operational parameters and tar yield

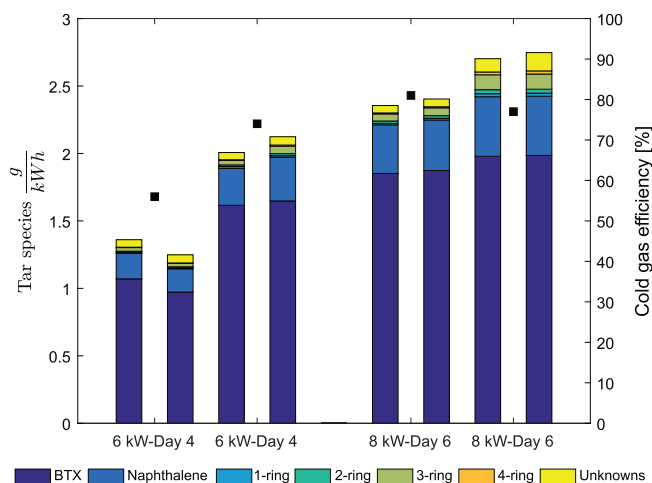It was observed that temperature was important for the tar yield. In

Fig. 6. Measured and identified tar amounts using LD slag as bed material in the 10 kW$_{th}$ reactor and using PFR as fuel at 970 °C. The measurements compare the repeats of the tar measurements at all points and also the effect of aging since the samples are from two different days with the same operational conditions. Cold gas efficiency (■) can be considered to be related to the oxygen transport to the fuel reactor.

Fig. 8 a summary of the tar results from experiments with LD slag is seen. In Fig. 8 two different fuels, PFR and BP, are compared at two different fuel loads at three different temperatures. It is observed that the tar amounts decrease with increased temperature and that a higher load increases the yield of tars. Using BP as a fuel generally generated higher amounts of tars compared to the using of PFR. A comparison to the reference material sand can be seen in supplementary material operated with 8 kW PFR at different temperatures. It can also be observed that the ratios of 3-ring and 4-ring compared to BTX are decreasing with increased temperatures at all conditions investigated. Branched 1-ring and 2-ring species was also observed to decrease with increased temperature for LD slag. This behavior is in direct contrast to what is known for sand [3] and is observed for ilmenite in Fig. 5. With sand, it was observed that increased 3-ring and 4-ring ratios with increased temperature, see supplementary material. The same trend can be seen when increasing the temperature for ilmenite with a higher yield of heavy tar products.

Besides temperature and load, the operation of CLG can be controlled by the circulation rate of the bed material. The circulation can be used to regulate the oxygen transfer to the fuel reactor and regulate the reduction degree of the oxygen carrier. Increasing the circulation to obtain higher effective oxygen to fuel ratio in the FR was evaluated and the results can be seen in Fig. 9. Increasing the overall lambda by increasing the circulation, indicated by the CI, only had a minor effect on the tar yield as can be seen in the figure. It was also observed that operating in conditions with very high circulation, closer to CLC (Chemical looping combustion) operation, the amounts of known tars were only decreased by ≈20 % compared to CLG operation with lower circulation. Same trend of tar yield was observed when comparing CLC and CLG operation with 6 kW BP at 870 °C. By increasing circulation, the ratios of 3-ring/BTX and 4-ring/BTX were increased slightly while using PFR as fuel; however, these ratios were almost unaffected while using straw as fuel.

Changing the steam ratio was observed to have a very limited effect on the tar components and amounts when the operation was performed with sand. The result can be seen in the supplementary material. No experiments with different steam ratios were performed with the different oxygen carriers.

3.2. Batch reactor tests with benzene

In Fig. 10 the conversion of benzene is displayed using either LD slag or ilmenite as an oxygen carrier with different concentrations of gasification gas at different temperatures. Here it can be observed that LD slag and ilmenite perform similarly when no other reducing gases are present. However, when reducing gases are introduced, the conversion of benzene decreases for both oxygen carriers, since H_2 and CO are known to inhibit tar reformation [40,41]. The conversion decreases more for LD slag than Ilmenite. Nevertheless, at higher temperatures, such as 950 °C, the difference between the two oxygen carriers is negligible.

To investigate if it is the reduction state of the oxygen carrier or the presence of other reducing gases that affects the benzene conversion, the two oxygen carriers were reduced before the benzene introduction. This was done with 50 % CO in N_2 and from the resulting CO_2 generation the oxidation state of the oxygen carrier, before the benzene introduction, could be calculated. The result can be observed in Fig. 11. Benzene was introduced to the reactor without gasification gas, corresponding to 0 % Gasification gas in Fig. 10.

It is clear that benzene conversion in this setup is related to the oxygen level ω of the oxygen carrier, for both oxygen carriers. However, the benzene conversion with LD slag decreased much faster than ilmenite. But LD slag indicated an increased conversion at more reduced states. It was noticed that the LD slag generated more H_2 than ilmenite during the reduction period with steam and benzene, an indication of water-splitting since the conversion of benzene was lower than with ilmenite. It was also noted that Ilmenite generated mainly CO_2 and some
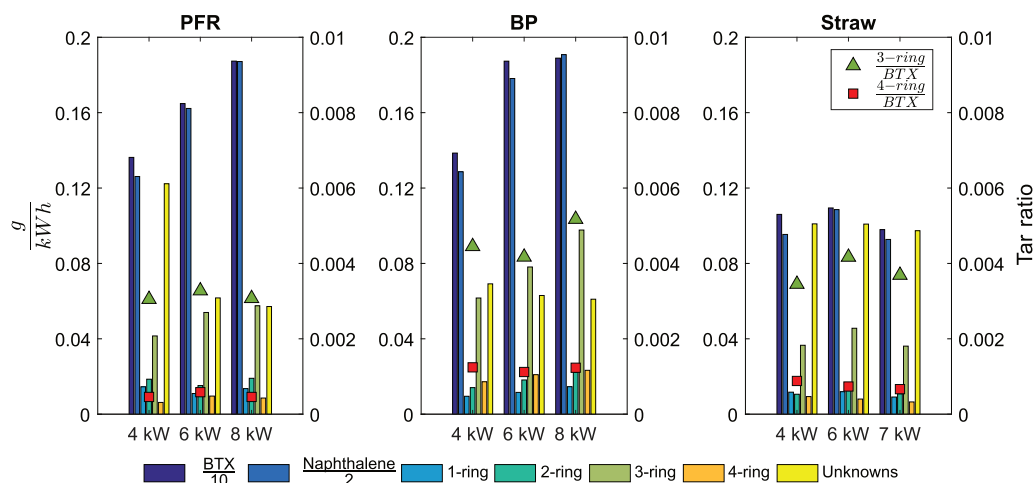
Fig. 7. Measured and identified tar amounts using LD slag as bed material in the 10 kW$_{th}$ reactor system and the effect of fuel load and fuel at 970 °C. It is observed that the total amounts of tar increase within increased fuel load. Observe that both BTX and naphthalene are divided by 10 respectively 2 to be able to see the other tar species better in the figure.
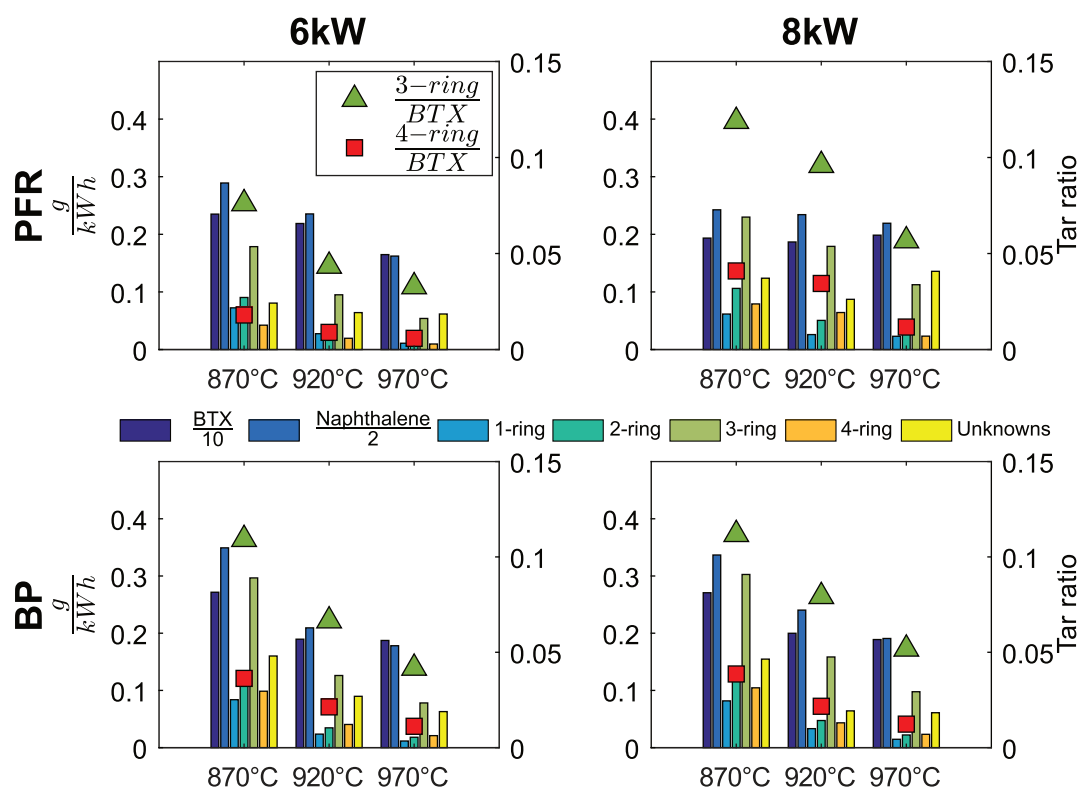

Fig. 8. Left axis in subplots: Measured and identified tar amounts using LD slag as bed material in the 10 kW$_{th}$ reactor system. Right axis in subplots: The ratios of identified 3-ring and 4-ring towards BTX. The temperature, fuel and fuel load are given in the figure. Generally, the amount of tars decreased at higher temperatures as well as the 3-ring and 4-ring ratio. Observe that both BTX and naphthalene are divided by 10, and 2, respectively, to be able to see the other tar species better in the figure.

CO besides H_2, while LD slag generated more or less only CO_2 and H_2. This was observed for LD slag no matter the length of the pre-reduction or the temperature.

4. Discussion

CLG could be a viable technology for the production of syngas with negative CO_2 emissions if carbon capture from the plant is intended since all generated CO_2 can be concentrated together with the syngas in

the FR. Another advantage, in comparison to normal indirect gasification, is that lower amounts of tars could be formed, due to the presence of the active bed material. In this study effects of operating parameters of CLG on tar formation were comprehensively investigated using ilmenite and LD slag as bed material in 10 kW$_{th}$ unit, and the results were compared to indirect gasification using sand as the bed material. From the results of this paper, it is observed that using oxygen carriers as bed material decreases the amount of tar formation compared to the case where sand was used as bed material. This is in coherence with previous
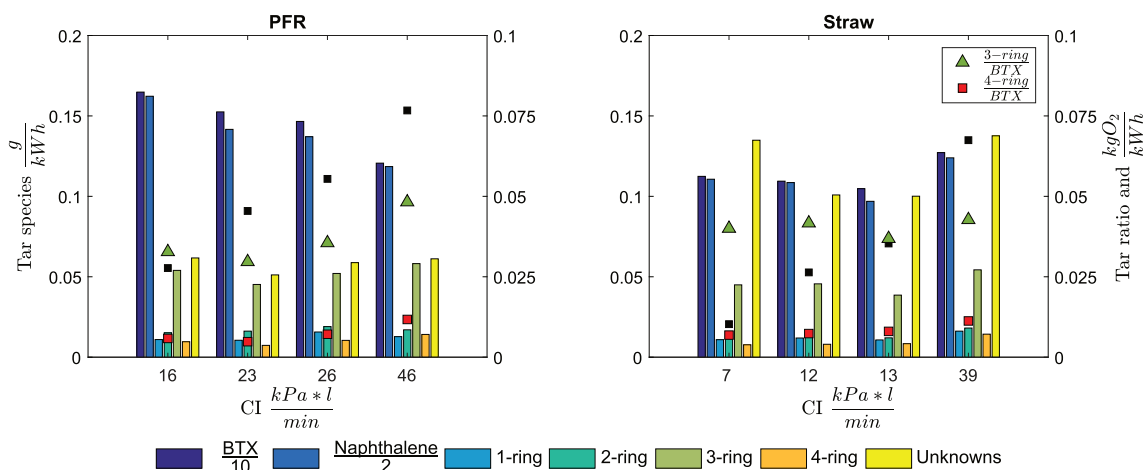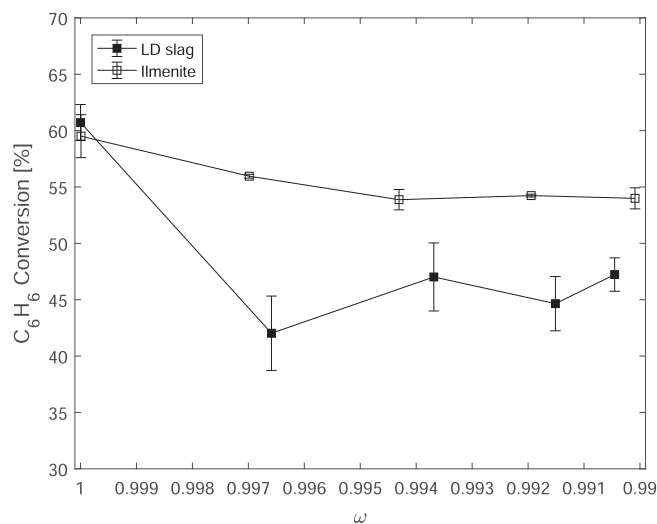
Fig. 9. Measured and identified tar amounts using LD slag as bed material in the 10 kW reactor system applying different circulation to obtain different λ in the fuel reactor. Left: The reactor was operated with PFR as fuel with a fuel rate of 6 kW at 970 °C. Right: The reactor was operated with Straw as fuel with a fuel rate of 6 kW at 970 °C. Observe that both BTX and naphthalene are divided by 10 respectively 2 to be able to see the other tar species better in the figure. On the right axis, the oxygen consumption in the AR by the oxygen carrier is indicated in the plot as ■ given in kgO₂/kWh – This is related to the actual oxygen transport to the fuel reactor by the oxygen carrier. 3-ring and 4-ring ratios towards BTX are shown in the figure also.
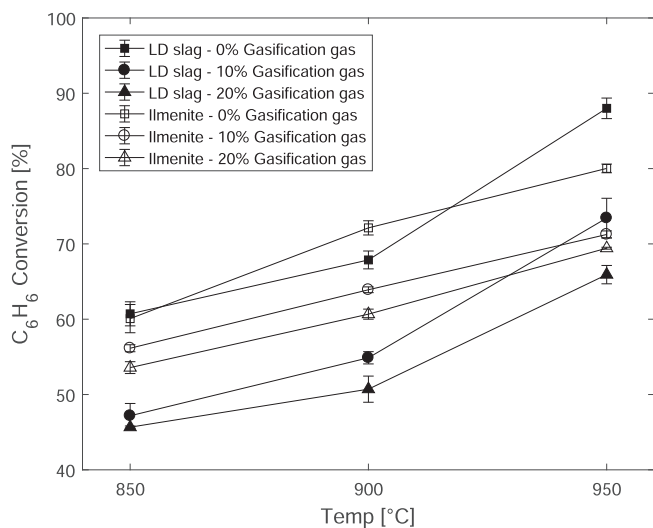
Fig. 10. Benzene conversion using LD slag or ilmenite as an oxygen carrier at different temperatures. The benzene was either introduced only with steam and nitrogen or together with a mixture of gasification gas. Numbers in the label are indicating the volumetric flow of the N2 and/or gasification gas (Gas-gas).

Fig. 11. Conversion of benzene using LD slag or ilmenite as an oxygen carrier reduced to different oxidation levels (ω) before benzene introduction at 850 °C.

studies [1,23] where oxygen carriers have been used as bed materials for gasification. Also, it is suggested that the amount of tars is less for LD slag compared to ilmenite, which also has been indicated in previous studies [23].

In downstream processes, heavy condensing tars are the cause of tar-related problems. As indicated in this and earlier studies using ilmenite [1], ilmenite has displayed a tendency to form a larger share of heavy tars compared to LD slag, see Fig. 5. However, the nonidentified large peak for ilmenite that had longer residence time in the GC than Crysene/Triphenylene is not included in the ratio. Since these heavy tars increase the dew point of the tar this could lead to operational issues [42]. The observed lower ratio of high 3-ring and 4-ring tar species for LD slag compared to ilmenite and sand may not only be due to oxygen transport to the fuel reactor. This is also indicated in Fig. 9, where the composition and tar yield are hardly affected by increased circulation to obtain higher oxygen transport to the fuel reactor. This can also be seen in batch experiments with benzene where, after initial reduction, the

conversion is almost the same independent of the reduction state, see Fig. 11. Ilmenite and LD slag converts benzene equally, and including other gaseous components, as seen in Fig. 10, affect the benzene conversion in the same way. This indicates that the lower tar yield observed from 10 kW$_{th}$ experiments are related to conversion of tar precursors, rather than conversion of the formed poly-aromatic compounds.

Ca and K are elements in bio ash that are recommended to be used as additives in large-scale gasification to promote catalytic reactions to decrease tar formation [43]. Larson *et al.* [43] emphasize in the review of six large-scale DFB gasifiers that the availability of active components in the bed, such as catalytic species, governs the impact on gas quality regarding composition and tar yields. K is a volatile catalyst acting mainly on char particles promoting the gasification of the char [44] and has some effect on the breaking of organic chains [45]. Ca species are non-volatile and are known to catalyze the water–gas-shift reaction but also enhance the breaking of organic chains and crack tar [44]. MgO alone and together with CaO [44,46] and CaO together with iron [44,47] have also been shown to have a catalytic effect on the cracking of tars species. LD slag contains a significant amount of Ca, both in

species like CaO but mostly as $(CaO)_xSiO_2$ and $Ca_2Fe_{3-x}A_xO_5$ besides $Mg_{1-x}Fe_xO$ [20,48]. LD slag is also known to have a limited capability of forming stable K-phases compared to sand and ilmenite [20,24]. This could also be indicated by the unaffected tar yield while using different loads of straw as fuel which contains a high amount of alkali compared to the other fuels, see Fig. 8. This combination of the release of volatile catalyst and high concentration of non-volatile catalyst phases present in LD slag can be the origin of the lower tar yields while using LD slag as bed material as could be observed in e.g. Fig. 5. This could suggest that LD slag is a good alternative to avoid issues related to condensing tars downstream in CLG.

Temperature is known to affect the polymerization reactions to generate higher amounts of polyaromatic tar species [3,42]. The temperature effect was also seen with sand as bed material, as seen in supplementary material with higher ratios of 3-ring and 4-ring in comparison to BTX when operated with PFR. The same trend was observed while using ilmenite as a bed material, generating higher ratios of 4-ring/BTX when the temperature increased from 870 °C to 970 °C, see Fig. 5. However, while using LD slag as a bed material, the ratios of 3-ring and 4-ring in comparison to BTX decreased, as seen in Fig. 8. This was observed for both PFR and BP at both 6- and 8-kW loads. This further indicates that LD slag either cracks higher tar species or prevents the polymerization reaction of tars. Instead, parts of the volatile tar species such as benzene are oxidized by LD slag, mainly generating CO_2 and H_2 as suggested by the batch experiments seen in Fig. 11.

An effect of aging of the LD slag particles was also observed on the tar yield, seen in Fig. 6. By aging LD slag higher amount of tar was generated, although cold gas efficiency was almost the same. Also, the ratio of 3-ring and 4-ring tars in relation to BTX was almost doubled with aging LD slag. This indicates that ash interaction, material degradation due to redox cycles, or a combination of both affect the generation and conversion of higher tar species. This has also been observed in our previous study, i.e. that aged material from boiler operation has a lower conversion towards benzene [20]. Studies using olivine have shown that ash coatings containing Ca increase the conversion of both light hydrocarbons and aromatics [49] besides reforming 1H-indene preventing polymerization into polycyclic aromatics [50]. This could indicate that active elements in the ash are less active than fresh LD slag.

Increasing fuel load has almost a proportional increase in tar yield, see Fig. 7. Therefore, it could be concluded that there is an issue with the fuel-oxygen carrier mixing. Also, the composition of the tar was similar at different fuel loads with more or less unaffected 3-ring and 4-ring ratios. The volatiles tar species do not interact fully with the bed material even in the new fuel reactor design with a volatile distributor. However, since no reference tar experiments were performed, the improvement from the old reactor design can't be quantified. Nevertheless, comparisons of the naphthalene concentrations from the raw syngas of the 2–4 MW_{th} gasifier operated with sand and ilmenite can be made. In 2–4 MW_{th} gasifier operated with sand and ilmenite, a naphthalene concentration of roughly 3.5–5 g/kg_{daf} at operation at 820–830 °C where measured [1]. In the 10 kW_{th} CLG pilot operation at 870 °C with 8 kW PFR and bed material of either i) sand: 3.6 g/kg_{fuel}, ii) Ilmenite: 3.4 g/kg_{fuel} and iii) LD slag: 2.4 g/kg_{fuel}, of naphthalene were obtained. This comparison is not for direct validation since the systems are operated at different temperatures and are very different in their layout. However, it gives an idea that with the same measurement technique the order of magnitude of naphthalene are the same for the two different systems.

The type of fuel affected the measured tars generated from the gasification. Tar yield from PFR and BP were both increasing with increased fuel load, while the tar yield was constant while using straw, see Fig. 7. This was expected to originate from the high alkali concentration in straw. Alkali is a known catalyst reducing tar formation in both lab-scale [25,39] and large scale operations [6]. When comparing PFR and BP in the same figure, it can be observed that less heavy tars (3-ring and 4-ring) were observed while using PFR.

The conversion of benzene in batch experiments is decreasing while the materials are reduced and other reducing gases are present. Inhibition of H_2 and CO on the tar cracking reaction is well established [40,41] and could be the reason why other gasification gases affect the tar conversion seen in Fig. 10, besides occupying oxidation sites. The decrease when the particles were reduced as in Fig. 11 could indicate that the conversion of benzene is partly to oxidation rather than catalytic cracking. However, the conversion of benzene indicated a slight increase when LD slag was further reduced. This has also been indicated in previous studies that iron at lower oxidation levels is more active toward benzene than at higher oxidation levels [51]. However, in CLC or CLG where the presence of steam is significant, it is not expected that LD slag will be reduced by more than 1.2 wt% [24]. Nevertheless, from TGA analysis of the bed samples in the FR from this operation, the omega was determined to be 0.989 to 0.996 (no yet published data) during operation in CLG mode. That is close to the region where the batch experiments were executed.

5. Conclusion

In this study, CLG operation was conducted using LD slag and ilmenite in a continuous 10 kW_{th} dual fluidized bed system. Sand was also used as a reference. From the raw syngas, tar samples were successfully collected and analyzed to identify how the bed material was affecting the tar conversion and composition. In addition, these results were compared to batch experiments using benzene as a reference tar component. From these experiments, it could be concluded:

- Oxygen carriers reduce the amount of tar in a gasification system.
- Benzene and Naphthalene are the main components of the tar that is detected using SPA columns.
- CLG operation using LD slag might result in lower absolute tar yield compared to ilmenite and sand.
- Oxygen transfer only had a minor effect on the tar yield in the FR.
- CLG operation using LD slag result in a lower ratio of heavy tars compared to ilmenite and sand.
- LD slag possesses catalytic properties towards tar reforming, both by not capturing volatile potassium from the fuel and containing a high amount of Ca that both catalyzes cracking of tars and prevents polymerization.
- Temperature and fuel load have a much larger effect on the tar yield than the circulation rate and steam ratio.
- Increasing temperature results in a lower ratio of 3-ring and 4-ring compounds in tars from CLG operation with LD slag, this is in direct contrast to what is seen and known with sand.
- The alkali content in the fuel seems to affect the tar generated from the gasification. Using Straw generated a considerably lower amount of tar and the tar generated was not affected by load, compared to PFR and BP.

CRediT authorship contribution statement

Fredrik Hildor: Conceptualization, Software, Methodology, Investigation, Writing – original draft, Writing – review & editing, Visualization. **Amir H Soleimanisalim:** Conceptualization, Methodology, Investigation, Writing – review & editing. **Martin Seemann:** Validation, Resources. **Tobias Mattisson:** Funding acquisition, Supervision. **Henrik Leion:** Funding acquisition, Supervision.

Declaration of Competing Interest

Data availability

Data will be made available on request.

Acknowledgment

Appendix A. Supplementary data

Supplementary data to this article can be found online at https://doi.org/10.1016/j.fuel.2022.125770.

References

[1] Larsson A, Israelsson M, Lind F, Seemann M, Thunman H. Using ilmenite to reduce the tar yield in a dual fluidized bed gasification system. Energy Fuels 2014;28(4):2632–44.

[2] Corella J, Aznar MP, Delgado J, Martinez MP, Aragües JL. The deactivation of tar cracking stones (dolomites, calcites, magnesites) and of commercial methane steam reforming catalysts in the upgrading of the exit gas from steam fluidized bed gasifiers of biomass and organic wastes. Stud Surf Sci Catal 1991;68(C):249–52.

[3] Milne TA, Evans RJ, "Biomass Gasifier ' Tars ': Their Nature , Formation , and Conversion," 1998.

[4] Heyne S, Harvey S. Assessment of the energy and economic performance of second generation biofuel production processes using energy market scenarios. Appl Energy 2013;101:203–12.

[5] Gassner M, Maréchal F. Thermo-economic process model for thermochemical production of Synthetic Natural Gas (SNG) from lignocellulosic biomass. Biomass Bioenergy 2009;33(11):1587–604.

[6] Larsson A, Gunnarsson I, Tengberg F, "The GoBiGas Project - Demonstration of the Production of Biomethane from Biomass via Gasification," 2018.

[7] Dieringer P, Marx F, Alobaid F, Ströhle J, Epple B. Process control strategies in chemical looping gasification-A novel process for the production of biofuels allowing for net negative CO2 emissions. Appl Sci (Switzerland) Jun. 2020;10(12):4271.

[8] Abad A. Chemical looping for hydrogen production. In: Calcium and Chemical Looping Technology for Power Generation and Carbon Dioxide (CO2) Capture. Woodhead Publishing; 2015. p. 327–74.

[9] Fan LS. Chemical Looping Systems for Fossil Energy Conversions. John Wiley & Sons Ltd; 2010.

[10] Moldenhauer P, Linderholm C, Rydén M, Lyngfelt A. Avoiding CO2 capture effort and cost for negative CO2 emissions using industrial waste in chemical-looping combustion/gasification of biomass. Mitig Adapt Strat Glob Change 2019;25(1):1–24.

[11] Leion H, Mattisson T, Lyngfelt A. Solid fuels in chemical-looping combustion. Int J Greenhouse Gas Control 2008;2(2):180–93.

[12] Keller M, Leion H, Mattisson T, Lyngfelt A. Gasification inhibition in chemical-looping combustion with solid fuels. Combust Flame 2011;158(3):393–400.

[13] Bayarsaikhan B, et al. Inhibition of steam gasification of char by volatiles in a fluidized bed under continuous feeding of a brown coal. Fuel 2006;85(3):340–9.

[14] Fushimi C, Wada T, Tsutsumi A. Inhibition of steam gasification of biomass char by hydrogen and tar. Biomass Bioenergy 2011;35(1):179–85.

[15] Yu Z, et al. Iron-based oxygen carriers in chemical looping conversions: A review. Carbon Resour Convers 2019;2(1):23–34.

[16] Matzen M, Pinkerton J, Wang X, Demirel Y. Use of natural ores as oxygen carriers in chemical looping combustion: A review. In: International Journal of Greenhouse Gas Control. Elsevier Ltd; 2017. p. 1–14.

[17] Fredrik L, et al. 12,000 hours of operation with oxygen-carriers in industrially relevant scale. VGB PowerTech 2017;7.

[18] Störner F, Lind F, Rydén M. Oxygen carrier aided combustion in fluidized bed boilers in Sweden—review and future outlook with respect to affordable bed materials. Appl Sci (Switzerland) 2021;11(17):7935.

[19] Rydén M, Hanning M, Lind F. Oxygen Carrier Aided Combustion (OCAC) of Wood Chips in a 12 MWth Circulating Fluidized Bed Boiler Using Steel Converter Slag as Bed Material. Appl Sci 2018;8(12):2657.

[20] Hildor F, Mattisson T, Leion H, Linderholm C, Rydén M. Steel converter slag as an oxygen carrier in a 12 MWth CFB boiler – Ash interaction and material evolution. Int J Greenhouse Gas Control 2019;88:321–31.

[21] Hildor F, Leion H, Linderholm CJ, Mattisson T. Steel converter slag as an oxygen carrier for chemical-looping gasification. Fuel Process Technol 2020;210:106576.

[22] Hedayati A, Soleimanisalim AH, Mattisson T, Lyngfelt A. Thermochemical conversion of biomass volatiles via chemical looping: Comparison of ilmenite and steel converter waste materials as oxygen carriers. Fuel 2022;313:122638.

[23] Pissot S, Berdugo Vilches T, Maric J, Seemann M. Chemical looping gasification in a 2–4 MWth dual fluidized bed gasifier. 23rd International Conference on Fluidized Bed Conversion. 2018.

[24] Störner F, Hildor F, Leion H, Zevenhoven M, Hupa L, Rydén M. Potassium Ash Interactions with Oxygen Carriers Steel Converter Slag and Iron Mill Scale in Chemical-Looping Combustion of Biomass-Experimental Evaluation Using Model Compounds. Energy Fuels 2020;34(2):2304–14.

[25] Mishima M, Suzuki T, Watanabe Y. Steam gasification of oil coke catalyzed by alkali metal hydridotetracarbonylferrates: Effects of alkali metal cations. Fuel Process Technol 1987;16(1):45–53.

[26] Jones JM, Darvell LI, Bridgeman TG, Pourkashanian M, Williams A. An investigation of the thermal and catalytic behaviour of potassium in biomass combustion. Proc Combust Inst 2007;31 II(2):1955–63.

[27] Jensen A, Dam-Johansen K, Wójtowicz MA, Serio MA. TG-FTIR study of the influence of potassium chloride on wheat straw pyrolysis. Energy Fuels 1998;12 (5):929–38.

[28] Li X, Lyngfelt A, Mattisson T. An experimental study of a volatiles distributor for solid fuels chemical-looping combustion process. Fuel Process Technol 2021;220:378–3820.

[29] Adánez J, Abad A, Mendiara T, Gayán P, de Diego LF, García-Labiano F. Chemical looping combustion of solid fuels. Prog Energy Combust Sci 2018.

[30] Lyngfelt A. Chemical-looping combustion of solid fuels - Status of development. Appl Energy 2014;113:1869–73.

[31] Mattisson T, et al. Chemical-looping technologies using circulating fluidized bed systems: Status of development. Fuel Process Technol 2018;172:1–12.

[32] Gogolev I, Soleimanisalim AH, Linderholm C, Lyngfelt A. Commissioning, performance benchmarking, and investigation of alkali emissions in a 10 kWth solid fuel chemical looping combustion pilot. Fuel 2020;119530.

[33] Pissot S, Vilches TB, Thunman H, Seemann M. Dual fluidized bed gasification configurations for carbon recovery from biomass. Energy Fuels 2020;34(12):16187–200.

[34] Israelsson M, Seemann M, Thunman H. Assessment of the solid-phase adsorption method for sampling biomass-derived tar in industrial environments. Energy Fuels 2013;27(12):7569–78.

[35] Berdugo Vilches T, Marinkovic J, Seemann M, Thunman H. Comparing Active Bed Materials in a Dual Fluidized Bed Biomass Gasifier: Olivine, Bauxite, Quartz-Sand, and Ilmenite. Energy and Fuels, Jun 2016;30(6):4848–57.

[36] Leion H, Frick V, Hildor F. Experimental Method and Setup for Laboratory Fluidized Bed Reactor Testing. Energies 2018;11(10):2505.

[37] Adánez J, Cuadrat A, Abad A, Gayán P, Diego LFD, García-Labiano F. Ilmenite activation during consecutive redox cycles in chemical-looping combustion. Energy Fuels 2010;24(2):1402–13.

[38] Corcoran A, Marinkovic J, Lind F, Thunman H, Knutsson P, Seemann M. Ash properties of ilmenite used as bed material for combustion of biomass in a circulating fluidized bed boiler. Energy Fuels 2014;28(12):7672–9.

[39] Pant KK, Kunzru D. Catalytic pyrolysis of n-heptane on unpromoted and potassium promoted calcium aluminates. Chem Eng J 2002;87(2):219–25.

[40] Jess A. Catalytic upgrading of tarry fuel gases: A kinetic study with model components. Chem Eng Process Process Intensif 1996;35(6):487–94.

[41] Devi L, Ptasinski KJ, Janssen FJJG. Pretreated olivine as tar removal catalyst for biomass gasifiers: Investigation using naphthalene as model biomass tar. Fuel Process Technol 2005;86(6):707–30.

[42] Li C, Suzuki K. Tar property, analysis, reforming mechanism and model for biomass gasification-An overview. no. 3. In: Renewable and Sustainable Energy Reviews. Pergamon; 2009. p. 594–604.

[43] Larsson A, Kuba M, Berdugo Vilches T, Seemann M, Hofbauer H, Thunman H. Steam gasification of biomass – Typical gas quality and operational strategies derived from industrial-scale plants. Fuel Process Technol 2021;212.

[44] Arnold RA, Hill JM. Catalysts for gasification: A review. Sustain Energy Fuels 2019;3(3):656–72.

[45] Devi L, Ptasinski KJ, Janssen FJJG. A review of the primary measures for tar elimination in biomass gasification processes. no. 2. In: Biomass and Bioenergy. Pergamon; 2003. p. 125–40.

[46] Delgado J, Aznar MP, Corella J. Biomass Gasification with Steam in Fluidized Bed: Effectiveness of CaO, MgO, and CaO-MgO for Hot Raw Gas Cleaning. Ind Eng Chem Res 1997;36(5):1535–43.

[47] Torres C, Rostom S, de Lasa H. An eco-friendly fluidizable Fex oy /cao-γ-al2 o3 catalyst for tar cracking during biomass gasification. Catalysts 2020;10(7):806.

[48] Waligora J, Bulteel D, Degrugilliers P, Damidot D, Potdevin JL, Measson M. Chemical and mineralogical characterizations of LD converter steel slags: A multi-analytical techniques approach. Mater Charact 2010;61(1):39–48.

[49] Kuba M, Havlik F, Kirnbauer F, Hofbauer H. Influence of bed material coatings on the water-gas-shift reaction and steam reforming of toluene as tar model compound of biomass gasification. Biomass Bioenergy 2016;89:40–9.

[50] Kuba M, Kirnbauer F, Hofbauer H. Influence of coated olivine on the conversion of intermediate products from decomposition of biomass tars during gasification. Biomass Convers Biorefin 2017;7(1):11–21.

[51] Tamhankar SS, Tsuchiya K, Riggs JB. Catalytic cracking of benzene on iron oxide-silica: catalyst activity and reaction mechanism. Appl Catal 1985;16(1):103–21.